Optical Heterodyne Detection Technique for Densely Multiplexed Millimeter-Wave-Band Radio-on-Fiber Systems

Toshiaki Kuri, *Member, IEEE,* and Ken-ichi Kitayama, *Fellow, IEEE*

Invited Paper

***Abstract*—Even in millimeter-wave-band (mm-wave-band) radio-on-fiber (ROF) systems, wavelength-division multiplexing (WDM) combined with subcarrier multiplexing (SCM) is a practical and attractive way to increase the channel capacity in existing optical-frequency-interleaved fibers. In this paper, we propose a channel selection scheme for interleaved dense WDM/SCM mm-wave-band ROF signals that use optical heterodyne detection with dual-mode local light. The principle underlying this scheme is explained theoretically, and channel selection of the DWDM/SCM ROF signal after transmission over a 25-km-long standard single-mode optical fiber has been experimentally demonstrated.**

***Index Terms*—Chromatic fiber dispersion, dense wavelength-division multiplexing (DWDM), dual-mode local light, laser phase noise, millimeter wave, optical heterodyne detection, radio-on-fiber (ROF), subcarrier multiplexing (SCM).**

NOMENCLATURE

A. List of Parameters

$e_x(t[,L])$	Amplitude of the optical signal or electrical (voltage) signal.
a_k	Amplitude of the kth order component of the optical signal.
P_x	Power of the optical signal.
f_x	Central frequency of the optical or electrical signal.
Δf	Central-frequency difference of the optical signal and local light.
ϕ_x	Phase noise of the optical carrier.
$\Delta\phi$	Phase-noise difference of the optical signal and local light.
$\varphi_{x(,k)}(t[,L])$	Phase (of the kth order component) of the optical or electrical signal.
$\varphi_{\mathrm{lo,LSB}}(t)$	Phase of the lower sideband component of dual-mode local light.
$\varphi_{\mathrm{lo,USB}}(t)$	Phase of the upper sideband component of dual-mode local light.
$i_x(t)$	Amplitude of the electrical (current) signal.
L	Fiber length.
$\beta(f)$	Propagation constant.
D	Fiber-dispersion parameter.
λ	Wavelength in fiber.
c	Velocity of light in a vacuum.
$\mathcal{R}$	O/E responsivity.
$-e$	Electron charge.
α	O/E sensitivity.
n_{sp}	Spontaneous emission coefficient.
B_{RF}	Occupied bandwidth of one SCM RF signal.
B	Total bandwidth of an SCM RF signal.
N	Maximum number of DWDM channels.
M	Maximum number of SCM channels.

B. List of Subscripts

$x = c$	Optical carrier from BS.
$x = s$	Modulated optical signal.
$x =$lo	Optical carrier for dual-mode local light.
$x =$RF	RF signal.
$x =$LO	Electrical local oscillator.
$x =$PD	Photocurrent.
$x =$IF	IF signal.
n	Number of DWDM channel.
m	Number of SCM channel.

I. INTRODUCTION

IN future wireless access networks, a millimeter-wave-band (mm-wave-band) radio-on-fiber (ROF) system will meet the demands for wider service coverage, broader bandwidth service, and larger channel capacity. It will also be a solution to the frequency scarcity of the commercial frequency resource.

Since the 1990s, many mm-wave-band ROF systems have been studied [1]–[29]. For initial deployment, a simple and low-cost base-station (BS) design is desirable [30]. This can be realized by putting all the ROF complexities into the central station (CS) and by sharing the cost over the BSs. This concept also enables the ease of maintenance and quick upgradability of entire systems. We have investigated various 60-GHz-band ROF systems [31]–[42], and have concluded that for mm-wave-band ROF systems, an external modulation

Manuscript received April 25, 2003; revised September 4, 2003.

T. Kuri is with the Basic and Advanced Research Division, Communications Research Laboratory, 184-8795 Tokyo, Japan (e-mail: kuri@crl.go.jp).

K. Kitayama is with the Graduate School of Engineering, Osaka University, 565–0871 Osaka, Japan (e-mail: kitayama@comm.eng.osaka-u.ac.jp).

Digital Object Identifier 10.1109/JLT.2003.821729

technique is one of the best ways to achieve the desired BS design.

To increase the channel capacity in existing optical fibers, wavelength-division multiplexing (WDM) combined with subcarrier multiplexing (SCM) is a practical and attractive means, as shown in Fig. 1. A variety of WDM ROF systems [43]–[47], SCM ROF systems [48]–[55], and WDM/SCM ROF systems [56]–[58] have been studied. Recently, to further increase optical spectral efficiency, dense WDM (DWDM) has also been investigated [45], [46]. In WDM or optical frequency-division multiplexing (FDM), individual optical carriers are modulated by radio-frequency (RF) signals and multiplexed in the optical domain. In SCM, on the other hand, the RF subcarriers are multiplexed in the electrical domain and multiplexed onto an optical carrier. In our SCM or DWDM mm-wave-band ROF systems [33], [59]–[62], we have focused on retaining a simple BS architecture. In these systems, narrow-band optical filters, such as, fiber Bragg grating (FBG) or arrayed waveguide grating (AWG), are used to demultiplex DWDM ROF signals. However, it is extremely difficult to realize an RF filter with a bandwidth of less than 1 GHz, which will be the typical bandwidth required in future wireless access.

Kikuchi *et al.* recently reported an experimental demonstration of the selection of any one of DWDM signals (called optical-FDM signals in [63], [64]) with an optical heterodyne receiver for optical baseband data transmission [63], [64]. This technique is based on an "FDM concept"; that is, fine frequency separation with an optical heterodyne receiver [65]. An optical heterodyne detection technique might also be an alternative for selecting DWDM ROF channels. Based on this expectation, we have proposed an optical heterodyne detection technique for an optical signal modulated by a subcarrier [66]–[68]. Optical heterodyning for subcarrier-modulated optical signals has been reported and investigated [69], [70]. In mm-wave-band ROF systems, however, it is difficult to use the conventional optical heterodyne detection with remote "single-mode" local light either because signal processing in the RF-band or a higher frequency range is required, or because an optical phase-locked loop (OPLL) is required. Therefore, we use a novel optical heterodyne detection technique for an ROF signal with remote "dual-mode" local light [66]–[68]. Our technique enables signal processing that can be done in a lower frequency range, such as in the conventional microwave band. Novel channel selection schemes have also been proposed for DWDM ROF systems [71] and SCM ROF systems [72]. To our knowledge, though, there has been no channel selection scheme for ultradense multiplexed ROF signals that uses anything like our optical heterodyne detection technique.

The distinctive features of our proposed channel selection scheme for a DWDM/SCM ROF system are as follows.

1) Channel selection for multiplexed ROF signals: In the proposed technique where remote dual-mode local light is used, selection of any one of the optical signals modulated by subcarriers, that is, multiplexed ROF signals, is distinguished from [63], where it is used to select any one of the optical signals modulated by baseband data.
2) Finely tunable filtering: By tuning the frequency of remote local light, the photodetected signals can be adjusted to a desired frequency range for the subsequent signal processing (for example, demodulation) [63], [66]–[68]. This will lead to finer frequency separation [65].
3) Use of an optical narrow bandpass filter (BPF) is unnecessary: The tunability and narrow-band electrical filters mean that an optical BPF with a narrow bandwidth is not needed to select a desired signal.
4) IF-band signal processing: The frequency conversion of heterodyning enables signal processing in an intermediate-frequency (IF) band (such as microwave or a lower frequency band) rather than in an RF band (such as mm-wave or a higher frequency band) [66]–[68]. This will help to reduce the need for expensive RF components.
5) Robustness regarding the chromatic fiber-dispersion effect: Since dual-mode local light is used, only two components (carrier and one of the first-order sideband components) are used for the detection, where the ROF signal generally has a double sideband (DSB) format. This refers to the same effect as detecting an optical single sideband (SSB) signal with the carrier, resulting in fiber-dispersion tolerance [66]–[68].
6) Insensitivity to laser phase noise: In principle, a phase-noise-canceling (PNC) function can be used to remove the laser phase noise [66]–[69].
7) High receiver sensitivity: The receiver sensitivity in optical heterodyne detection systems is expected to be higher than that in optical direct detection systems because it is hard in practice to achieve an ideal noise figure of 3 dB in optical amplifiers [66]–[68], [70], [73]. Moreover, even if optical amplifiers are used in an optical link, a 3-dB improvement in system performance is theoretically expected because only one polarization component—which has the same polarization as the local light—is detected in the optical heterodyne detection [70]. Here, note that an amplified spontaneous emission noise has random polarization.
8) Reduction of optical noise sources: The high receiver sensitivity means that optical amplifiers can be eliminated or their number can be reduced [66]–[68], [70]. This contributes to the high system performance.
9) No OPLLs: Our technique does not need OPLLs for the purpose of frequency stabilization of the local light [65] because of the PNC function [66]–[69].

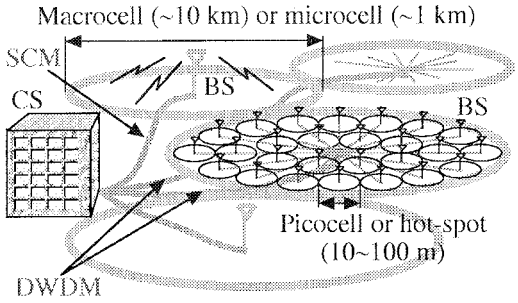

Fig. 1. Multiplexed ROF systems.

To confirm the validity of the principle underlying our technique, we have experimentally demonstrated transmission over

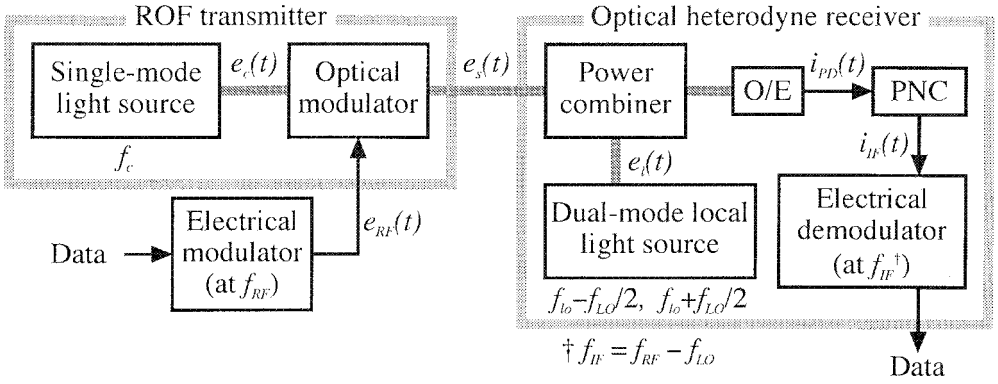

Fig. 2. Fundamental configuration of the optical heterodyne detection system using a dual-mode local light source.

a 25-km-long standard single-mode fiber (SMF) and channel selection of four channels, which consisted of two 25-GHz-spaced DWDM optical carriers, each individually modulated by two 60-GHz-band carriers with 155.52-Mb/s differential phase-shift keying (DPSK) data.

II. Principle

A. Optical Heterodyne Detection of a Single ROF Signal

Fig. 2 shows a fundamental block diagram of the optical heterodyne detection system using a dual-mode local light source [67]. The transmitter is a conventional mm-wave-band ROF generator, generally consisting of a single-mode light source and an external optical modulator. The optical heterodyne receiver consists of a dual-mode local light source, an optical power combiner, an optical-to-electrical converter (O/E), a PNC circuit, and an electrical demodulator.

An optical carrier from the single-mode light source $e_c(t)$ is expressed as

$$e_c(t) \propto \sqrt{2P_c} \cdot \exp\{j\varphi_c(t)\} \tag{1}$$

$$\varphi_c(t) = 2\pi f_c t + \phi_c(t) \tag{2}$$

where P_c, f_c, and $\phi_c(t)$ are the power, the center frequency, and the phase noise of the optical carrier, respectively. Let an RF signal at the output of an electrical modulator $e_{\rm RF}(t)$ be written as

$$e_{\rm RF}(t) = V_{\rm RF} \cdot \exp\{j\varphi_{\rm RF}(t)\} \tag{3}$$

$$\varphi_{\rm RF}(t) = 2\pi f_{\rm RF} t + \theta(t) \tag{4}$$

where $V_{\rm RF}$, $f_{\rm RF}$, and $\theta(t)$ represent the amplitude, the carrier frequency, and the phase-modulated data of the RF signal, respectively. The above RF signal is assumed to be phase-modulated in order to overcome the radio fading problem. The optical carrier $e_c(t)$ is modulated by the RF signal $e_{\rm RF}(t)$ and transmitted over an optical link. Taking into account the fiber-dispersion effect, the modulated optical signal after the propagation in an optical fiber of length L is generally written as

$$\begin{aligned} e_s(t,L) &\propto \sqrt{2P_c} \cdot \sum_{k=-\infty}^{\infty} a_n \cdot e^{j\varphi_{s,n}(t,L)} \\ &\simeq \sqrt{2P_c}\left[a_{-1}e^{j\varphi_{s,-1}(t,L)} + a_0 e^{j\varphi_{s,0}(t,L)} + a_1 e^{j\varphi_{s,1}(t,L)}\right] \end{aligned} \tag{5}$$

and

$$\begin{aligned} \varphi_{s,k}(t,L) &= \varphi_c(t) + k\varphi_{\rm RF}(t) - \beta(f)\cdot L \\ &\simeq 2\pi(f_c + kf_{\rm RF})(t - \beta_1 L) + k\theta(t - \beta_1 L) \\ &\quad + \phi_c(t - \beta_1 L) - \frac{1}{2}\beta_2 (2\pi k f_{\rm RF})^2 \cdot L \\ &\quad + (2\pi f_c \cdot \beta_1 - \beta_0)\cdot L. \end{aligned} \tag{6}$$

With Taylor expansion at f_c, we used the approximation of the propagation constant $\beta(f)$ written as follows [74]:

$$\beta(f) \simeq \beta_0 + \beta_1 2\pi(f - f_c) + \frac{1}{2}\beta_2\{2\pi(f - f_c)\}^2. \tag{7}$$

In (6), $\beta_1 L$ corresponds to the group delay time and $\beta_2 = -\lambda^2 D/2\pi c$ is satisfied, where D, λ, and c are the fiber-dispersion parameter, the wavelength in the fiber, and the velocity of light in a vacuum, respectively. Note that the last term in (6) is constant and independent of time, and the second-to-last term represents the fiber-dispersion effect.

A free-running dual-mode light source having a frequency separation of $f_{\rm LO}$ is used to detect the ROF signal. Here, the dual-mode light source is considered to have frequency separation that is either highly stabilized or jitter-free, and is written as

$$e_l(t) \propto \sqrt{P_{\rm lo}} \cdot \left\{e^{j\varphi_{\rm lo,LSB}(t)} + e^{j\varphi_{\rm lo,USB}(t)}\right\} \tag{8}$$

$$\varphi_{\rm lo,LSB}(t) = 2\pi\left(f_{\rm lo} - \frac{f_{\rm LO}}{2}\right)t + \phi_{\rm lo}(t) \tag{9}$$

$$\varphi_{\rm lo,USB}(t) = 2\pi\left(f_{\rm lo} + \frac{f_{\rm LO}}{2}\right)t + \phi_{\rm lo}(t) \tag{10}$$

where $P_{\rm lo}$, $f_{\rm lo}$, and $\phi_{\rm lo}(t)$ are the power, the center frequency, and the phase noise of the dual-mode local light, respectively. The dual-mode local light is combined with the received optical signal, as shown in Fig. 3(a). We assume that the polarizations of the received optical signal and the optical local reference are matched. The photocurrent $i_{PD}(t)$ then becomes

$$\begin{aligned} i_{PD}(t) &= \mathcal{R}\sqrt{2P_c P_{\rm lo}}a_{-1}e^{j(\varphi_{s,-1}(t,L) - \varphi_{\rm lo,LSB}(t))} \\ &\quad + \mathcal{R}\sqrt{2P_c P_{\rm lo}}a_0 e^{j(\varphi_{s,0}(t,L) - \varphi_{\rm lo,USB}(t))} \\ &\quad + \mathcal{R}\sqrt{2P_c P_{\rm lo}}a_{-1}e^{j(\varphi_{\rm lo,USB}(t) - \varphi_{s,-1}(t,L))} \\ &\quad + \mathcal{R}P_{\rm lo}e^{j2\pi f_{\rm LO}t} + 2\mathcal{R}P_c a_0 a_{-1}e^{j\varphi_{\rm RF}(t - \beta_1 L)} \\ &\quad + \cdots. \end{aligned} \tag{11}$$

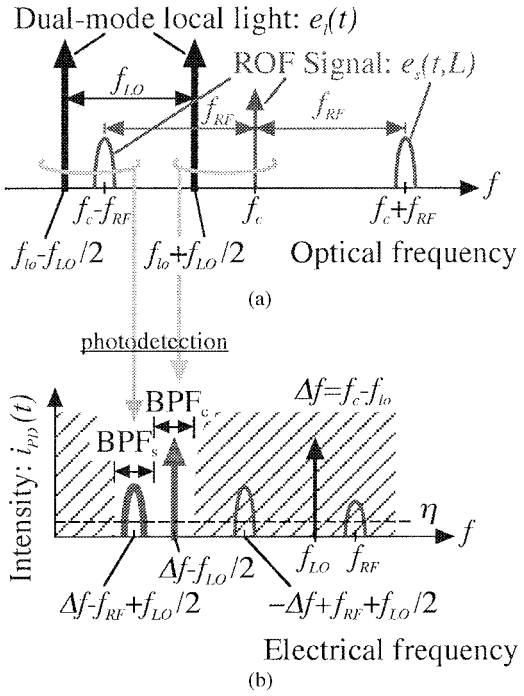

Fig. 3. (a) Optical spectra of signal $e_s(t, L)$ and local $e_l(t)$. (b) Electrical spectra at the O/E output.

Note that $\mathcal{R}$ is the O/E responsivity. Fig. 3(b) shows the spectrum of $i_{PD}(t)$. We focus on two phase components

$$\varphi_{s,-1}(t,L)-\varphi_{\mathrm{lo,LSB}}(t)=2\pi\left(\Delta f-f_{\mathrm{RF}}+\frac{f_{\mathrm{LO}}}{2}\right)(t-\beta_1 L)+\theta(t-\beta_1 L)-\frac{1}{2}\beta_2(2\pi f_{\mathrm{RF}})^2 L+\{2\pi f_s\beta_1-\beta_0\}L+\Delta\phi(t,L) \quad (12)$$

$$\varphi_{s,0}(t,L)-\varphi_{\mathrm{lo,USB}}(t)=2\pi\left(\Delta f-\frac{f_{\mathrm{LO}}}{2}\right)(t-\beta_1 L)+\{2\pi f_{\mathrm{lo}}\beta_1-\beta_0\}L+\Delta\phi(t,L) \quad (13)$$

where

$$\Delta f\equiv f_c-f_{\mathrm{lo}} \quad (14)$$

$$\Delta\phi(t,L)\equiv\phi_c(t-\beta_1 L)-\phi_{\mathrm{lo}}(t). \quad (15)$$

Fig. 4 shows one of the possible PNC configurations. In the PNC, the two components at $\Delta f-f_{\mathrm{RF}}+f_{\mathrm{LO}}/2$ and $\Delta f-f_{\mathrm{LO}}/2$ are separated by electrical bandpass filters (BPF$_s$ and BPF$_c$). They are multiplied by each other, and then the signal down-converted to f_{IF}, $i_{\mathrm{IF}}(t)$, is filtered out by BPF$_{\mathrm{IF}}$

$$i_{\mathrm{IF}}(t)\propto\mathcal{R}^2P_cP_{\mathrm{lo}}a_0a_{-1}e^{j\varphi_{\mathrm{IF}}(t,L)} \quad (16)$$

$$\varphi_{\mathrm{IF}}(t,L)=\{\varphi_{s,-1}(t,L)-\varphi_{\mathrm{lo,LSB}}(t)\}-\{\varphi_{s,0}(t,L)-\varphi_{\mathrm{lo,USB}}(t)\}=2\pi f_{\mathrm{IF}}(t-\beta_1 L)+\theta(t-\beta_1 L)-\left\{\beta_0-2\pi f_{\mathrm{IF}}\beta_1+\frac{1}{2}\beta_2(2\pi f_{\mathrm{RF}})^2\right\}L \quad (17)$$

$$f_{\mathrm{IF}}\equiv f_{\mathrm{RF}}-f_{\mathrm{LO}}. \quad (18)$$

From the above, we can discuss the features below. First, no laser phase-noise term remains in (16) or (17). This means

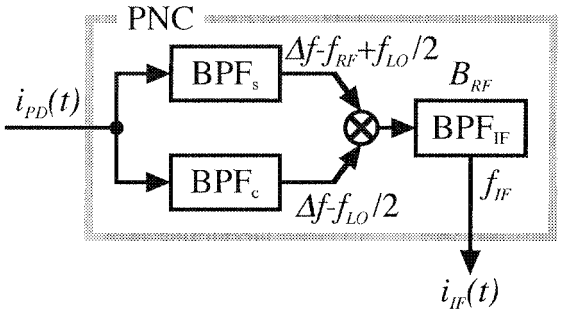

Fig. 4. A possible PNC configuration.

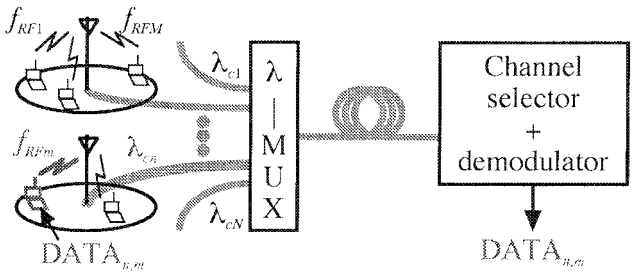

Fig. 5. Channel selection scheme.

that this detection technique is, in principle, free from laser phase noise. Second, the last term in (17) represents the phase delay for a fiber length of L and is constant. If the RF signal is DPSK-encoded, the fiber-dispersion effect does not seriously affect the transmission quality because only two optical components—i.e., one single-sideband (SSB) component and carrier—are detected. Third, the filtering to select the desired signal components is performed within the electrical domain rather than in the optical domain. Since the frequency stability and controllability of lasers have recently progressed in conjunction with the development of DWDM technologies, this technique will be able to provide fine and tunable filtering of the desired optical components by using conventional electrical filters.

Let us consider the theoretical system performance of the optical heterodyne detection receiver. Under the local shot-noise limited environment, the theoretical signal-to-noise power ratio (SNR) is given by [67], [68]

$$\frac{S}{N}=\frac{1}{2}\cdot\frac{\alpha P_c}{B}\cdot\frac{a_0^2a_{-1}^2}{a_0^2+a_{-1}^2} \quad (19)$$

where α [$=\mathcal{R}/e$, where $-e$ is the electron charge] and B_{RF} are the O/E sensitivity and the bandwidth of BPF$_{\mathrm{IF}}$, respectively. Similarly, under the same conditions, the theoretical SNR of conventional intensity modulation/direct detection with an optical amplifier is given by [67], [68]

$$\frac{S}{N}=\frac{1}{2n_{sp}}\cdot\frac{\alpha P_c}{B}\cdot\frac{a_0^2a_{-1}^2}{a_0^2+a_{-1}^2} \quad (20)$$

where n_{sp} is the spontaneous emission coefficient of the optical amplifier, which in practice is more than one. From these results, we can see that the SNR for optical heterodyne detection is improved by a factor of n_{sp}.

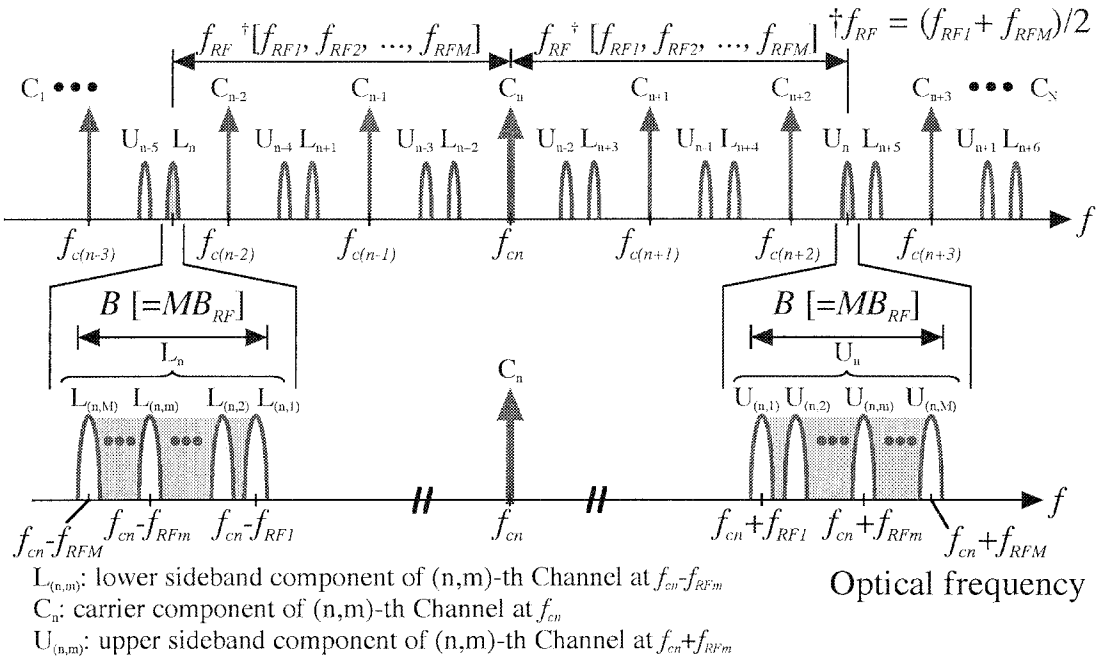

Fig. 6. Spectrum design of multiplexed ROF signal.

B. Channel Selection Scheme in Multiplexed ROF Systems

Fig. 5 illustrates the concept of the proposed channel selection scheme in a multiplexed ROF system. In our conceptual system configuration, a wavelength of λ_n ($n = 1, 2, \ldots, N$) is allocated to one of the BSs: BS$_n$. A radio terminal with the data of DATA$_{n,m}$ ($m = 1, 2, \ldots, M$) accesses the closest antenna in BS$_n$, where an RF carrier frequency of f_{RFm} is allocated to the radio terminal. In each BS, an ROF signal is modulated by a mm-wave-band SCM signal, consisting of M RF carriers with carrier frequencies of $f_{\mathrm{RF1}}, \ldots, f_{\mathrm{RFM}}$, and each with a bandwidth of B_{RF}. For convenience, we assume that f_{RF} [$= (f_{\mathrm{RF1}} + f_{\mathrm{RF}N})/2$] and B [$= M \cdot B_{\mathrm{RF}}$] are the center frequency and the total bandwidth of the SCM signal, respectively. To achieve higher optical-spectral efficiency, we introduced an optical frequency interleaving technique through a DWDM multiplexer (λ-MUX). Fig. 6 shows the spectrum design of the multiplexed ROF signal with the optical frequency interleaving. Each ROF signal has an optical double sideband (DSB) format in general. In Fig. 6, only three components of each ROF signal—the carrier (C_n), the first-order lower sideband (LSB, L_n), and the first-order upper sideband (USB, U_n)—are depicted because the higher order nonlinear components can be ignored in most practical cases. Here, L_n and U_n consist of sets of $\{L_{(n,1)}, \ldots, L_{(n,M)}\}$ and $\{U_{(n,1)}, \ldots, U_{(n,M)}\}$, respectively. The format may be an optical SSB signal, which consists of the carrier component (C_n) and one of the sideband components (L_n or U_n). If the optical SSB format is used, more efficient use of the optical frequency resource can be expected. Since our purpose in this paper is to show theoretically that the proposed channel selection scheme is suitable for the general case, the DSB format is considered below. The following theory, though, can be easily applied to the SSB format.

1) DWDM Channel Selection: To focus on our explanation of the DWDM channel selection, we assume that a single RF signal ($M = 1$) is received at the antenna in one BS. Fig. 7 shows the spectra when selecting the $(n, 1)$th channel. As shown in Fig. 7(a), the frequencies of a high-power dual-mode local light $f_{\mathrm{lo}n} - f_{\mathrm{LO1}}/2$ and $f_{\mathrm{lo}n} + f_{\mathrm{LO1}}/2$ are set to optically extract only two components of the LSB (L_n [$= L_{(n,1)}$]) and the carrier (C_n) [71]. The center frequency of the dual-mode local light $f_{\mathrm{lo}n}$ is tuned so that it equals Δf [$= f_{cn} - f_{\mathrm{lo}n}$] of (14). Optical heterodyning will cause many beat signals to appear at the O/E output, as shown in Fig. 7(a). However, the two desired components at $\Delta f - f_{\mathrm{RF1}} + f_{\mathrm{LO1}}/2$ and $\Delta f - f_{\mathrm{LO1}}/2$ can be extracted by BPF$_s$ and BPF$_c$ in the PNC (Fig. 4), where almost all undesired beat components are easily removed. As mentioned, the beat of two filtered components becomes a desired IF signal (f_{IF} [$= f_{\mathrm{RF1}} - f_{\mathrm{LO1}}$]) at the output of the PNC. Although some undesired components may remain in BPF$_s$ and/or BPF$_c$, undesired beats can also be removed by BPF$_{\mathrm{IF}}$ with the bandwidth B_{RF}, as shown in Fig. 7(c). Here, B_{RF} corresponds to the transmission bandwidth of one RF signal. In this way, the nth channel only can be selected. In the same manner, the other channel, the $(n', 1)$th channel, can also be extracted by tuning the central frequency of the dual-mode local light $f_{\mathrm{lo}n'}$. To successfully perform the channel selection, moreover, the spectrum of the DWDM ROF signal and the dual-mode local light should be carefully designed so that the undesired components do not drop into the passband of BPF$_{\mathrm{IF}}$. The details of this have been described more fully in [71].

2) SCM Channel Selection: To focus on explaining the SCM channel selection, here we consider single wavelength transmission ($N = 1$). Fig. 8 shows the spectra when the $(1, m)$th channel is selected. As shown in Fig. 8(a), the frequencies of a high-power dual-mode local light $f_{\mathrm{lo1}} - f_{\mathrm{LO}m}/2$ and $f_{\mathrm{lo1}} + f_{\mathrm{LO}m}/2$ are set to optically extract the LSBs

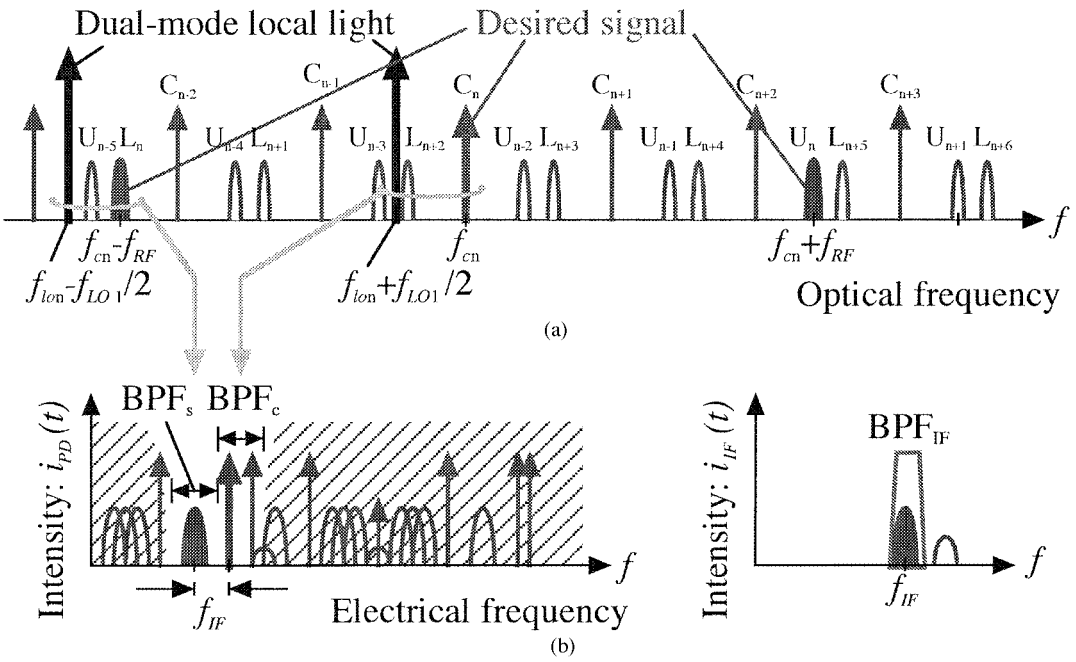

Fig. 7. (a) Local light to select the $(n,1)$th channel, (b) O/E output, and (c) PNC output.

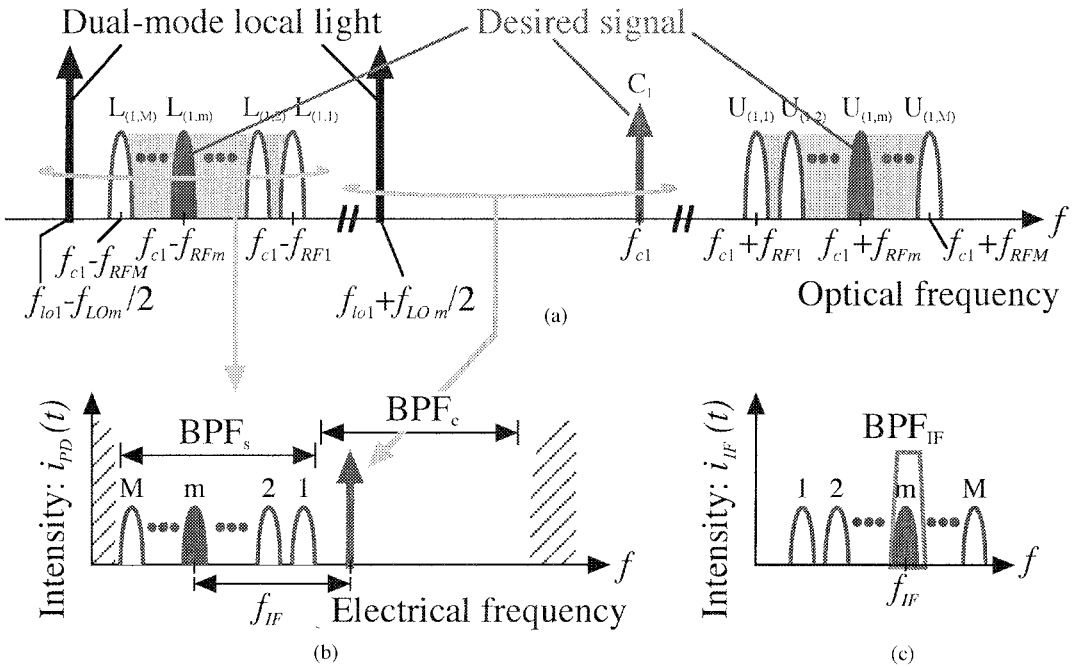

Fig. 8. (a) Local light to select the (1,m)th channel, (b) O/E output, and (c) PNC output.

$(L_{(1,1)},\ldots,L_{(1,M)})$ and the carrier (C_1). The center frequency of the dual-mode local light $f_{\rm lo1}$ is tuned so that it equals Δf $[=\ f_{c1}-f_{\rm lo1}]$ of (14). Next, $f_{{\rm LO}m}$ is tuned to satisfy $f_{\rm IF}$ $[=\ f_{{\rm RF}m}-f_{{\rm LO}m}]$ of (18), where $f_{\rm IF}$ is the target frequency for the subsequent demodulation. Optical heterodyning causes some beats $(i_{PD}(t))$, which come from C_1 and $\{L_{(1,1)},\ldots,L_{(1,M)}\}$, to appear at the O/E output, as shown in Fig. 8(b). Next, the signal and carrier parts, which are separated by BPF$_s$ and BPF$_c$, are multiplied by each other. Finally, a desired channel only can be extracted with BPF$_{\rm IF}$, as shown in Fig. 8(c). In this way, the (1,m)th channel only can be selected. In the same manner, the other channel, the (1,m')th channel, can also be extracted by tuning the mode interval of the dual-mode local light $f_{{\rm LO}m'}$.

3) DWDM/SCM Channel Selection: We applied our optical heterodyne detection technique to the DWDM/SCM system, as illustrated in Fig. 5. The DWDM/SCM channel selection can be done through a combination of the DWDM and SCM-channel selections. Let us consider the received DWDM/SCM signal shown in Fig. 6. For channel selection, the target channel is assumed to be the (n,m)th channel. First, the frequencies of a dual-mode local light $f_{{\rm lo}n}-f_{{\rm LO}m}/2$ and $f_{{\rm lo}n}+f_{{\rm LO}m}/2$

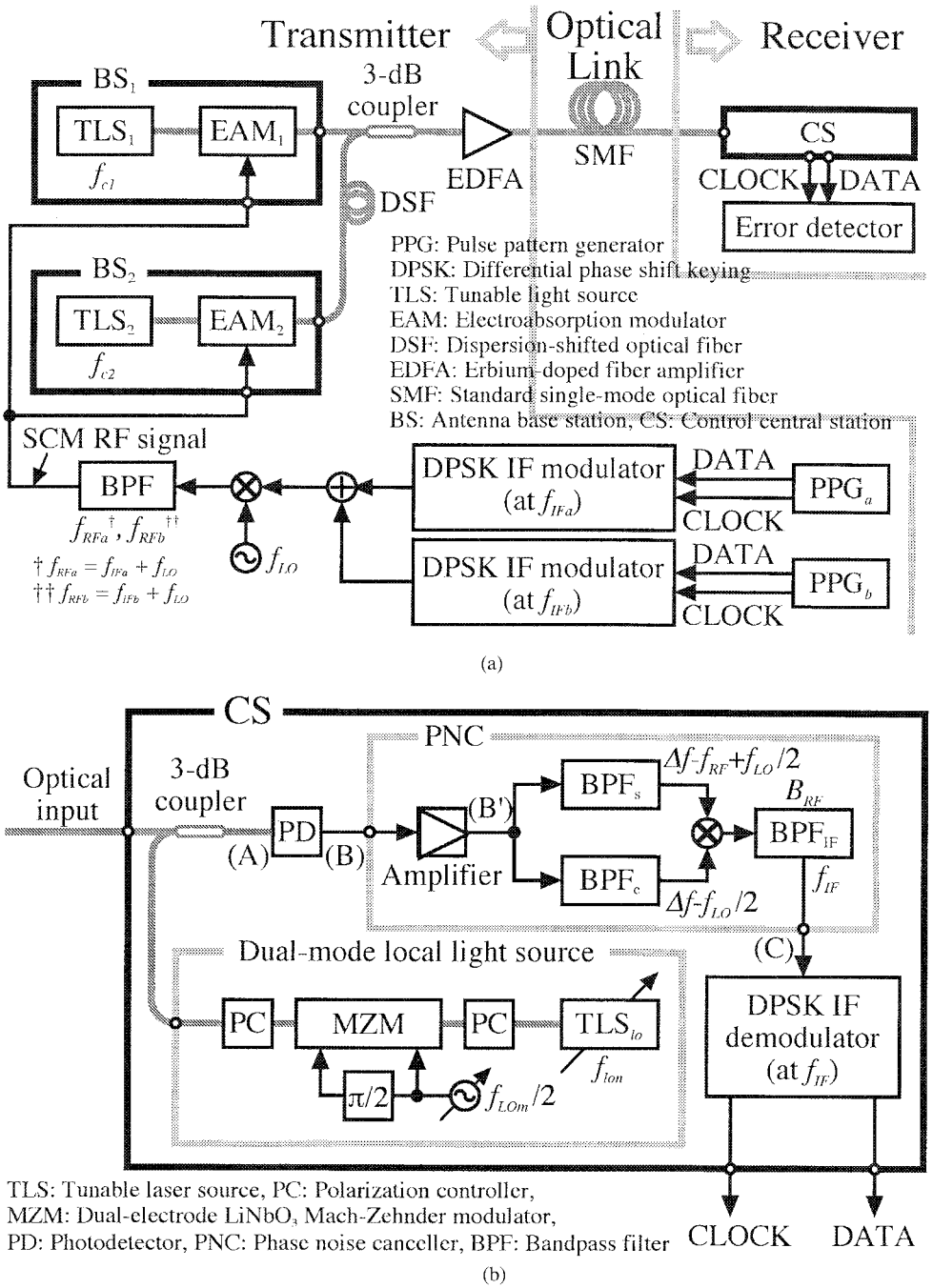

Fig. 9. (a) Experimental setup and (b) CS configuration.

are set to optically extract a group of LSBs (L_n) and the carrier (C_n). The center frequency and the mode interval of the dual-mode local light f_{lon} and f_{LOm} are tuned so that they equal Δf [$= f_{cn} - f_{\mathrm{lon}}$] and f_{IF} [$= f_{\mathrm{RF}m} - f_{\mathrm{LO}m}$]. The optical heterodyning causes beats ($i_{PD}(t)$), which come from C_n and $\{L_{(n,1)}, \ldots, L_{(n,M)}\}$, to appear at the O/E output, as similarly shown in Fig. 8(b) where the (1,m)th channel should be replaced by the (n,m)th channel.

Next, the signal and carrier parts separated by BPF_s and BPF_c are multiplied by each other. Finally, a desired channel only can be extracted with $\mathrm{BPF}_{\mathrm{IF}}$ in exactly the same way as shown in Fig. 8(c). In this way, the (n,m)th channel only can be selected. In the same manner, the other channel, the (n',m')th channel, can also be extracted by tuning both the central frequency and the mode interval of the dual-mode local light $f_{\mathrm{lon}'}$ and $f_{\mathrm{LO}m'}$.

III. Experimental Demonstration

A. Experimental Setup

To verify the effectiveness of our channel selection scheme, we performed an experiment. Fig. 9 shows the experimental setup for the proof-of-concept, where $N = 2$ and $M = 2$. In Fig. 9(a), two optical carriers from independent single-mode continuous-wave (CW) light sources (TLS_1 and TLS_2) with carrier frequencies of f_{c1} [$= c/\lambda_{c1}$, $\lambda_{c1} = 1550.12$ nm] and

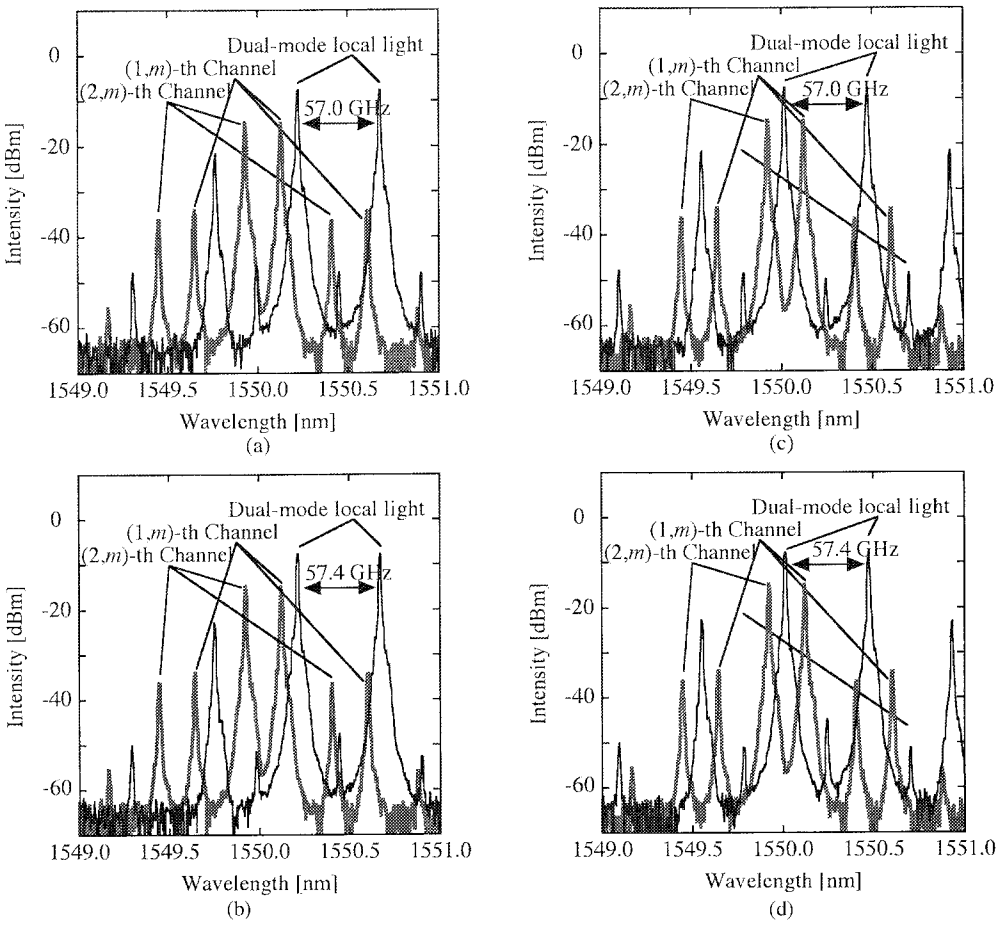

Fig. 10. Measured optical spectra at PD input for selection of (a) the (1,1)th channel, (b) the (1,2)th channel, (c) the (2,1)th channel, and (d) the (2,2)th channel.

f_{c2} [$= c/\lambda_{c2}$, $\lambda_{c2} = 1549.92$ nm] are individually modulated with an SCM RF signal with a 60-GHz-band electroabsorption modulator (EAM_1 and EAM_2). The SCM RF signal consisted of 59.6-GHz [$= f_{RF1}$] and 60.0-GHz [$= f_{RF2}$] carriers. The RF carriers were modulated by 155.52-Mb/s-DPSK, a $2^{23} - 1$ pseudo random bit sequence (PRBS) from a pulse pattern generator (PPG_a or PPG_b) via a DPSK IF modulator at 2.6 GHz [$= f_{IFa}$] or 3.0 GHz [$= f_{IFb}$], an electrical combiner, a mm-wave-band mixer, and a 57.0-GHz oscillator. The total power of the SCM RF signal applied to each EAM was -1 dBm. A 112-m-long dispersion-shifted fiber before a 3-dB optical coupler was used to decrease the correlation between the two optical signals. Two SCM ROF signals centered at 1550.12 and 1549.92 nm were power-combined by the 3-dB coupler, resulting in an optical-frequency-interleaved DWDM/SCM ROF signal. The channel space was 25 GHz [$= f_{c2} - f_{c1}$]. This signal was amplified by an erbium-doped fiber amplifier and then transmitted over a 25-km-long SMF to a remote CS that included an optical heterodyne receiver.

As shown in Fig. 9(b), the tunable dual-mode local light source consisted of another free-running single-mode CW light source (TLS_{lo}) with a carrier frequency of f_{lon}, two polarization controllers (PCs), a dual-electrode $LiNbO_3$ Mach–Zehnder modulator (MZM), and an electrical tunable local oscillator driven at $f_{LOm}/2$. The optical power of TLS_{lo} and the total RF power of the electrical local oscillator were 9.7 and 13.0 dBm, respectively. In the dual-mode local light source, f_{lon} and $f_{LOm}/2$ were tunable. To select the (1,m)th channel ($m = 1$ or 2), f_{lo1} was set to about $c/1550.45$ nm, and to select the (2,m)th channel, f_{lo2} was set to about $c/1550.25$ nm (Fig. 10). To select the (n,1)th channel ($n = 1$ or 2), f_{LO1} was set to 57.0 GHz, and to select the (n,2)th channel, f_{LO2} was set to 57.4 GHz. The MZM was set so that it acted as a carrier-suppressed DSB (DSB-SC) modulator. The local light and the DWDM signal were combined by another 3-dB optical coupler. The combined light was input to a photodetector (PD) and detected by means of optical heterodyning. The polarizations of the received signal and of the local light were optimized by two PCs to maximize the photocurrent. The photocurrent was then input to a PNC. The PNC consisted of an electrical amplifier, three BPFs (BPF_s, BPF_c, and BPF_{IF}), and an electrical mixer. BPF_s, BPF_c, and BPF_{IF} had 3-dB bandwidths of 2000, 2000, and 234 MHz at the central frequencies of 8.0, 11.0, and 2.6 GHz, respectively. The respective optimal 3-dB bandwidths of BPF_s and BPF_c, $B_{s.opt}$ and $B_{c.opt}$, are given by

$$B_{s.opt} = B + \kappa_c \Delta f_c + \kappa_{lo} \Delta f_{lo} \tag{21}$$

$$B_{c.opt} = \kappa_c \Delta f_c + \kappa_{lo} \Delta f_{lo}, \tag{22}$$

where Δf_c and Δf_{lo} are the linewidths of TLS_n ($n = 1, 2$) and TLS_{lo}, respectively. The extension coefficients κ_c and κ_{lo} are used to cope with the spectrum bandwidth broadening caused

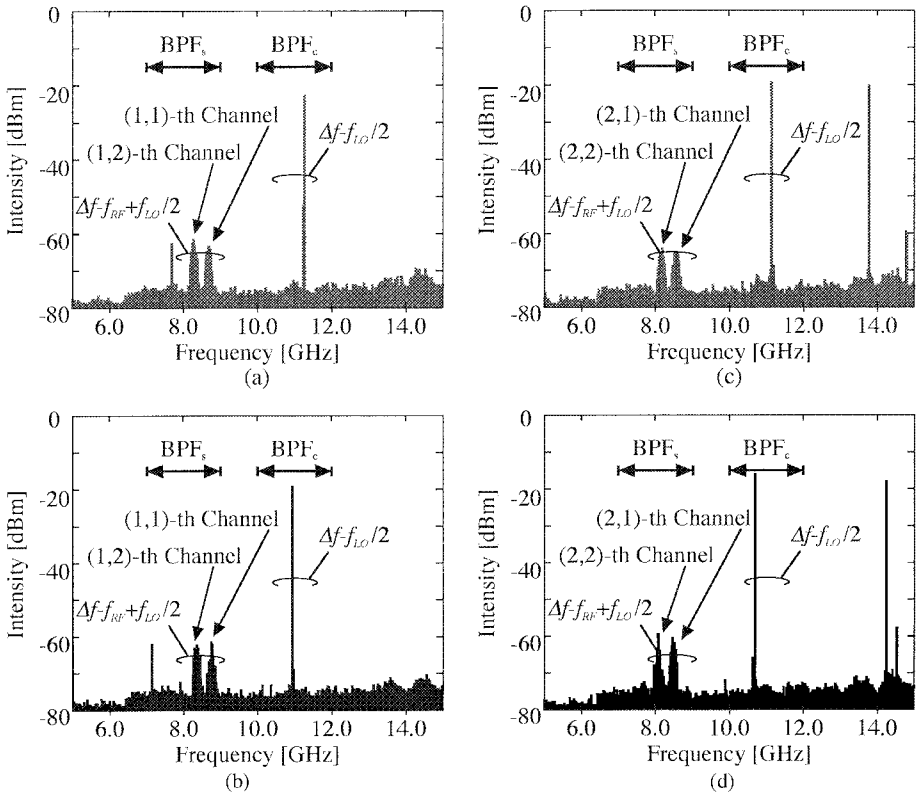

Fig. 11. Measured photocurrent for selection of (a) the (1,1)th channel, (b) the (1,2)th channel, (c) the (2,1)th channel, and (d) the (2,2)th channel.

by the phase noise and depend on the spectrum shape of the optical carrier [75]. The passbands of the mixer's RF-, LO-, and IF-ports were 6.0–18.0, 3.5–18.0, and dc–3.0 GHz, respectively. As mentioned, in the PNC, two parts of the photodetected components were filtered out by BPF$_s$ and BPF$_c$; these were multiplied by each other, and only a desired channel at 2.6 GHz [$= f_{\rm IF}$] was filtered out with BPF$_{\rm IF}$. Finally, the selected signal was demodulated by the DPSK IF demodulator, and then the bit error rate (BER) was measured with an error detector.

In our system, a remote-located light source technique, which is a technique for transmitting an optical carrier from the CS, can also be applied [35], [42]. In our concept, an optical amplifier (if necessary to compensate not only the transmission loss up to the λ-MUX but also the insertion loss of the λ-MUX) is located just after the λ-MUX shown in Fig. 5, and it can be shared by many users. Also, the light source located in the CS is used instead of an optical amplifier to compensate the transmission loss from the λ-MUX to the receiver (CS) [66]–[68]. This feature leads to reduction of optical noise sources.

B. Experimental Results

Fig. 10 shows the optical spectra measured at the PD input. The thick lines show the DWDM/SCM ROF signal and the thin lines show the dual-mode local light. The effective modulation indexes of two SCM ROF signals with optical carrier frequencies of 1550.12 and 1549.92 nm were 19 and 21 dB, respectively. The difference in the indices was due to the different characteristics of EAM$_1$ and EAM$_2$. Under all conditions of the dual-mode local light, the even-order components were well suppressed. Moreover, the intensity ratio between the first-order desired and the third-order undesired components of the dual-mode local light was about -15 dB [$= (J_3(x)/J_1(x))^2$, where $J_n(x)$ is the nth-order Bessel function], nearly corresponding to the condition for obtaining the theoretical maximum value of $|J_1(x)|$ given at $x = 1.84$. This shows that the MZM was driven under almost ideal conditions. Even in the ideal case, the third-order components, which are larger than $L_{(n,m)}$ and $U_{(n,m)}$, may affect the system performance through interchannel interference. Therefore, they should be suppressed when multiplexing a larger number of wavelengths. To overcome this problem, narrow bandpass filtering, the DBR mode-locked laser [13], or dual-mode injection locking [19] can be applied. In this proof-of-concept experiment, however, these components did not affect the system performance because they were not close to the signal components ($L_{(n,m)}$).

Fig. 11 shows the electrical spectrum of the photocurrent, which was measured at the point (B') in Fig. 9(b). For all cases, the two photodetected components ($\Delta f - f_{RFm} + f_{{\rm LO}m}/2$ and $\Delta f - f_{{\rm LO}m}/2$, $m = 1, 2$) successfully appeared at about 8.0 and 11.0 GHz, respectively, as expected. This shows that the central frequency of the dual-mode local light $f_{{\rm lo}n}$ was stably controllable with accuracy of ± 1 GHz, corresponding to ± 8 pm in the 1550-nm band, where the relative wavelength accuracy of the TLSs used in the experiment was ± 5 pm in the worst case. We also observed that the frequencies of all components caught by BPF$_s$ and BPF$_c$ fluctuated by about 100 MHz. This fluctuation was caused by the laser phase noise and the slow wavelength fluctuation, where the linewidth of the TLSs was less than 1 MHz.

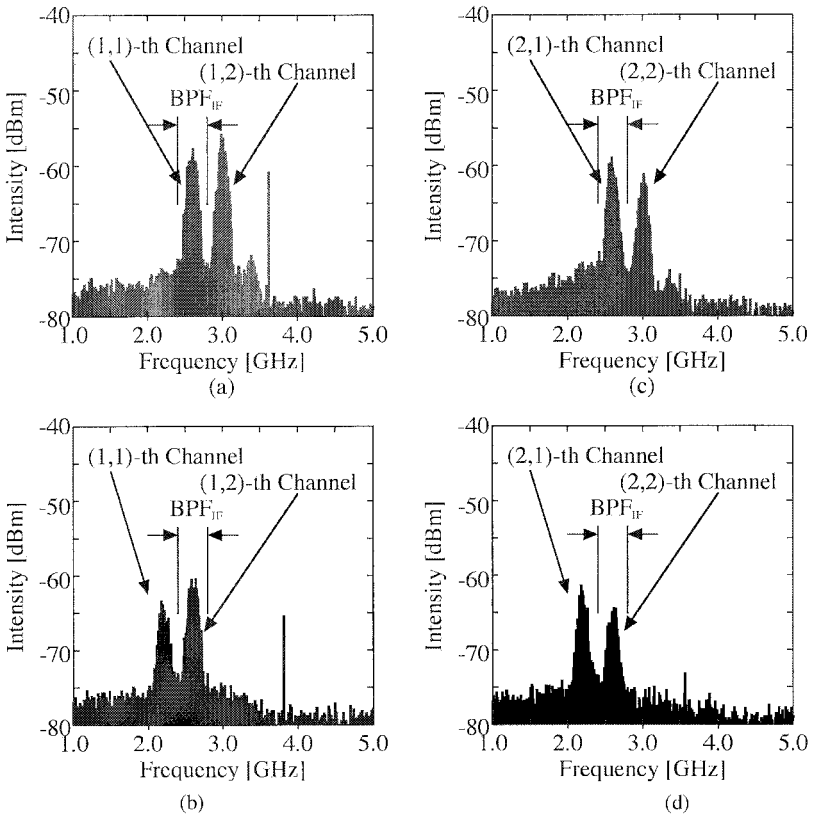

Fig. 12. Measured electrical spectra at the BPF_{IF} input for selection of (a) the (1,1)th channel, (b) the (1,2)th channel, (c) the (2,1)th channel, and (d) the (2,2)th channel.

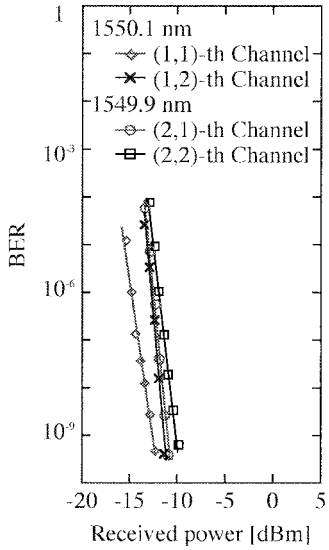

Fig. 13. Measured BERs.

Fig. 12 shows the electrical spectra measured at the input of BPF_{IF} in the PNC. It can be seen that the desired channel was successfully selected through the optical heterodyne detection without serious effects due to laser phase noise from the TLSs or chromatic fiber dispersion. Note that undesired components can be easily eliminated by BPF_{IF}. Some level differences in the measured IF signals were observed. Although it is difficult to identify the cause of these differences exactly, we think they were due to incomplete polarization matching and the different oscillating conditions of the dual-mode local light. Moreover, we confirmed that all IF signals without data were highly frequency-stable. The measured linewidth of all IF signals was less than -73 dBc/Hz at 10 kHz from the carrier. This shows that the laser phase noise was successfully cancelled.

To investigate the system performance, we also measured the BER for each channel after the 25-km-long SMF transmission. The results are plotted in Fig. 13. The BER of all four channels was less than 10^{-9} after the channel selection without any BER floor. Some differences in the receiver sensitivities were observed. These were due to both the polarization mismatch of the received optical signal and the adjustment error of the dual-mode local light. This result shows the practicality of our channel selection scheme for application to DWDM/SCM ROF systems.

IV. Conclusion

A novel channel selection scheme with optical heterodyne detection using dual-mode local light and the PNC function for DWDM/SCM ROF systems has been proposed. In this scheme, the channel selection is carried out by tuning both the center frequency and the frequency interval of dual-mode local light. The proposed scheme has a number of distinctive features:

1) channel selection for multiplexed ROF signals;
2) fine tunable filtering;
3) no optical narrow BPF needed;
4) IF-band signal processing;
5) fiber-dispersion tolerance;

6) laser phase-noise insensitivity;
7) high receiver sensitivity;
8) reduction of optical noise sources;
9) no OPLLs.

In the proof-of-concept experiment, selection of any of the optical-frequency-interleaved DWDM/SCM 60-GHz-band ROF signals with independent 155.52-Mb/s DPSK data after transmitting over a 25-km-long SMF was successfully demonstrated.

ACKNOWLEDGMENT

T. Kuri thanks N. Otani, T. Itabe, and T. Iida of the Communications Research Laboratory for their encouragement.

REFERENCES

[1] H. Ogawa, D. Polifko, and S. Banba, "Novel techniques for high-capacity 60-GHz fiber-radio transmission systems," *IEEE Trans. Microwave Theory Tech.*, vol. 40, pp. 2285–2293, Dec. 1992.

[2] D. Novak, Z. Ahmed, R. B. Waterhouse, and R. S. Tucker, "Signal generation using pulsed semiconductor lasers for application in millimeter-wave wireless links," *IEEE Trans. Microwave Theory Tech.*, vol. 43, pp. 2257–2262, Sept. 1995.

[3] D. Wake, C. R. Lima, and P. A. Davies, "Optical generation of millimeter-wave signals for fiber-radio systems using a dual-mode DFB semiconductor laser," *IEEE Trans. Microwave Theory Tech.*, vol. 43, pp. 2270–2276, Sept. 1995.

[4] E. Suematsu and N. Imai, "A fiber optic/millimeter-wave radio transmission link using HBT as direct photodetector and an optoelectronic upconverter," *IEEE Trans. Microwave Theory Tech.*, vol. 44, pp. 133–143, Jan. 1996.

[5] S. L. Zhang and J. J. O'Reilly, "Effect of dynamic stimulated Brillouin scattering on millimeter-wave fiber radio communication systems," *IEEE Photon. Technol. Lett.*, vol. 9, pp. 395–397, Mar. 1997.

[6] D. Wake, C. R. Lima, and P. A. Davies, "Transmission of 60-GHz signals over 100 km of optical fiber using a dual-mode semiconductor laser source," *IEEE Photon. Technol. Lett.*, vol. 8, pp. 578–580, Apr. 1996.

[7] L. Moura, M. Darby, P. M. Lane, and J. J. O'Reilly, "Impact of interferometric noise on the remote delivery of optically generated millimeter-wave signals," *IEEE Microwave Theory Tech.*, vol. 45, pp. 1398–1402, Aug. 1997.

[8] S. L. Zhang, P. M. Lane, and J. J. O'Reilly, "Assessment of the nonlinearity tolerance of different modulation schemes for millimeter-wave fiber-radio systems using MZ modulators," *IEEE Trans. Microwave Theory Tech.*, vol. 45, pp. 1403–1409, Aug. 1997.

[9] L. Noël, D. Wake, D. G. Moodie, D. D. Marcenac, L. D. Westbrook, and D. Nesset, "Novel techniques for high-capacity 60-GHz fiber-radio transmission systems," *IEEE Trans. Microwave Theory Tech.*, vol. 45, pp. 1416–1423, Aug. 1997.

[10] T. Hoshida and M. Tsuchiya, "Broad-band millimeter-wave upconversion by nonlinear photodetection using a waveguide p-i-n photodiode," *IEEE Photon. Technol. Lett.*, vol. 10, pp. 860–862, June 1998.

[11] A. Stöhr, K. Kitayama, and D. Jäger, "Full-duplex fiber-optic RF subcarrier transmission using a dual-function modulator/photodetector," *IEEE Trans. Microwave Theory Tech.*, vol. 47, pp. 1388–1341, July 1999.

[12] R. A. Griffin, H. M. Salgado, P. M. Lane, and J. J. O'Reilly, "System capacity for millimeter-wave radio-over-fiber distribution employing an optically supported PLL," *J. Lightwave Technol.*, vol. 17, pp. 2480–2487, Dec. 1999.

[13] T. Ohno, K. Sato, S. Fukushima, Y. Doi, and Y. Matsuoka, "Application of DBR Mode-locked lasers in millimeter-wave fiber-radio system," *J. Lightwave Technol.*, vol. 18, pp. 301–307, Jan. 2000.

[14] Y. Doi, S. Fukushima, T. Ohno, Y. Matsuoka, and H. Takeuchi, "Phase shift keying using optical delay modulation for millimeter-wave fiber-optic radio links," *J. Lightwave Technol.*, vol. 18, pp. 301–307, Mar. 2000.

[15] C. Lim, A. Nirmalathas, D. Novak, R. Waterhouse, and G. Yoffe, "Millimeter-wave broad-band fiber-wireless system incorporating baseband data transmission over fiber and remote LO delivery," *J. Lightwave Technol.*, vol. 18, pp. 1355–1363, Oct. 2000.

[16] A. Nirmalathas, D. Novak, C. Lim, and R. B. Waterhouse, "Wavelength reuse in the WDM optical interface of a millimeter-wave fiber-wireless antenna base station," *IEEE Trans. Microwave Theory Tech.*, vol. 49, pp. 2006–2012, Oct. 2001.

[17] T. Ohno, S. Fukushima, Y. Doi, Y. Muramoto, and Y. Matsuoka, "Transmission of millimeter-wave signals in a fiber-radio system using a uni-traveling-carrier waveguide photodiode," *IEEE Photon. Technol. Lett.*, vol. 12, pp. 1379–1381, Oct. 2000.

[18] X. Wang, N. J. Gomes, L. Gomez-Rojas, P. A. Davies, and D. Wake, "Indirect optically injection-locked oscillator for millimeter-wave communication system," *IEEE Microwave Theory Tech.*, vol. 48, pp. 2596–2603, Dec. 2000.

[19] M. Ogusu, K. Inagaki, Y. Mizuguchi, and T. Ohira, "If signal transmission at 60 GHz-band using direct modulation of a two-mode locked Fabry-Perot slave laser," *IEEE Microwave Wireless Comp. Lett.*, vol. 11, pp. 290–292, July 2001.

[20] L. A. Johansson and A. J. Seeds, "36-GHz 140-Mb/s radio-over-fiber transmission using an optical injection phase-lock loop source," *IEEE Photon. Technol. Lett.*, vol. 13, pp. 893–895, Aug. 2001.

[21] Y. Ozeki, K. Higuma, S. Oikawa, M. Kishi, and M. Tsuchiya, "A 60-GHz optoelectronic mixing scheme of high image and carrier rejection ratios with an integrated optical single-sideband modulator employed," *IEEE Microwave Theory Tech.*, vol. 49, pp. 1986–1991, Oct. 2001.

[22] H. Harada, K. Sato, and M. Fujise, "A radio-on-fiber based millimeter-wave road-vehicle communication system by a code division multiplexing radio transmission scheme," *IEEE Trans. Intell. Trans. Syst.*, vol. 2, pp. 165–179, Dec. 2001.

[23] C. Marra, A. Nirmalathas, D. Novak, C. Lim, L. Reekie, J. A. Besley, and N. J. Baker, "The impact of grating dispersion on transmission performance in a millimeter-wave fiber-radio system," *IEEE Photon. Technol. Lett.*, vol. 14, pp. 1345–1347, Sept. 2002.

[24] L. A. Johansson, C. P. Liu, and A. J. Seeds, "A 65-km span unamplified transmission of 36-GHz radio-over-fiber signals using an optical injection phase-lock loop," *IEEE Photon. Technol. Lett.*, vol. 14, pp. 1596–1598, Nov. 2002.

[25] C. Lim, D. Novak, A. Nirmalathas, and G. H. Smith, "Dispersion-induced power penalties in millimeter-wave signal transmission using multisection DBR semiconductor laser," *IEEE Microwave Theory Tech.*, vol. 49, pp. 288–296, Feb. 2001.

[26] Y. Doi, S. Fukushima, T. Ohno, and K. Yoshino, "Frequency stabilization of millimeter-wave subcarrier using laser heterodyne source and optical delay line," *IEEE Photon. Technol. Lett.*, vol. 13, pp. 1002–1004, Sept. 2001.

[27] G. Grosskopf, D. Rohde, R. Eggemann, S. Bauer, C. Bornholdt, M. Mohrle, and B. Sartorius, "Optical millimeter-wave generation and wireless data transmission using a dual-mode laser," *IEEE Photon. Technol. Lett.*, vol. 12, pp. 1692–1694, Dec. 2000.

[28] Y. Shoji and H. Ogawa, "Experimental demonstration of 622 Mbps millimeter-wave over fiber link for broadband fixed wireless access system," in *2002 Int. Topical Meeting Microwave Photonics (MWP2002) Tech. Dig.*, vol. F3–2, Awaji, Hyogo, Japan, Nov. 2002, pp. 367–370.

[29] A. Stöhr, C. Miesner, and D. Jäger, "All-optical radio-independent millimeter-wave radio-on-fiber system with lean antenna base stations," in *2002 Int. Topical Meeting Microwave Photonics (MWP2002) Tech. Dig.*, vol. P3–1, Awaji, Hyogo, Japan, Nov. 2002, pp. 213–216.

[30] K. Kitayama, "Architectural considerations on fiber radio millimeter-wave wireless access systems," *J. Fiber Integrat. Opt.*, vol. 19, pp. 167–186, 2000.

[31] T. Kuri and K. Kitayama, "60 GHz millimeter signal generation and transport over optical frequency division multiplexing networks," *Electron. Lett.*, vol. 32, no. 23, pp. 2158–2159, Nov. 1996.

[32] K. Kitayama and R. A. Griffin, "Optical downconversion from millimeter-wave to if-band over 50 km-long optical fiber link using an electroabsorption modulator," *IEEE Photon. Technol. Lett.*, vol. 11, pp. 287–289, Feb. 1999.

[33] T. Kuri, K. Kitayama, A. Stöhr, and Y. Ogawa, "Fiber-optic millimeter-wave downlink system using 60 GHz-band external modulation," *J. Lightwave Technol.*, vol. 17, pp. 799–806, May 1999.

[34] A. Stöhr, K. Kitayama, and T. Kuri, "Fiber-length extension in an optical 60-GHz transmission system using an EA-modulator with negative chirp," *IEEE Photon. Technol. Lett.*, vol. 11, pp. 739–741, June 1999.

[35] T. Kuri, K. Kitayama, and Y. Ogawa, "Fiber-optic millimeter-wave uplink system incorporating remotely fed 60-GHz-band optical pilot tone," *IEEE Trans. Microwave Theory Tech.*, vol. 47, pp. 1332–1337, July 1999.

[36] A. Stöhr, T. Kuri, K. Kitayama, R. Heinzelmann, and D. Jäger, "Full-duplex 60 GHz fiber-optic transmission," *Electron. Lett.*, vol. 35, no. 19, pp. 1653–1655, Sept. 1999.

[37] K. Kitayama, "Ultimate performance of optical DSB signal-based millimeter-wave fiber-radio system: Effect of laser phase noise," *J. Lightwave Technol.*, vol. 17, pp. 1774–1781, Oct. 1999.

[38] H. Sotobayashi and K. Kitayama, "Cancellation of the signal fading for 60 GHz subcarrier multiplexed optical DSB signal transmission in nondispersion shifted fiber using midway optical phase conjugation," *J. Lightwave Technol.*, vol. 17, pp. 2488–2497, Dec. 1999.

[39] T. Kuri, K. Kitayama, and Y. Takahashi, "60-GHz-band full-duplex radio-on-fiber system using two-RF-port electroabsorption transceiver," *IEEE Photon. Technol. Lett.*, vol. 12, pp. 419–421, Apr. 2000.

[40] K. Kitayama, A. Stöhr, T. Kuri, R. Heinzelmann, D. Jäger, and Y. Takahashi, "An approach to single optical component antenna base stations for broadband millimeter-wave fiber-radio access systems," *IEEE Trans. Microwave Theory Tech.*, vol. 48, pp. 2588–2595, Dec. 2000.

[41] T. Kamisaka, T. Kuri, and K. Kitayama, "Simultaneous modulation and fiber-optic transmission of 10-Gb/s baseband and 60-GHz-band radio signals on single wavelength," *IEEE Trans. Microwave Theory Tech.*, vol. 49, pp. 2013–2017, Oct. 2001.

[42] T. Kuri, K. Kitayama, and Y. Takahashi, "A single light source configuration for full-duplex 60-GHz-band radio-on-fiber system," *IEEE Trans. Microwave Theory Tech.*, vol. 51, pp. 431–439, Feb. 2003.

[43] C. G. Schäffer, M. Sauer, K. Kojucharow, and H. Kaluzni, "Increasing the channel number in WDM mm-wave systems by spectral overlap," in *2000 Int. Topical Meeting Microwave Photonics (MWP2002) Tech. Dig.*, vol. WE2.4, Oxford, U.K., Sept. 2000, pp. 164–167.

[44] D. Castleford, A. Nirmalathas, D. Novak, and R. S. Tucker, "Optical crosstalk in fiber-radio WDM networks," *IEEE Trans. Microwave Theory Tech.*, vol. 49, pp. 2030–2035, Oct. 2001.

[45] C. Lim, A. Nirmalathas, D. Novak, R. S. Tucker, and R. B. Waterhouse, "Technique for increasing optical spectral efficiency in millimeter-wave WDM fiber-radio," *Electron. Lett.*, vol. 37, no. 16, pp. 1043–1045, Aug. 2001.

[46] C. Lim, A. Nirmalathas, D. Novak, and R. B. Waterhouse, "Capacity analysis and optimum channel allocations for a WDM ring fiber-radio backbone incorporating wavelength interleaving with a sectorized antenna interface," in *2002 Int. Topical Meeting Microwave Photonics (MWP2002) Tech. Dig.*, vol. F3–3, Awaji, Hyogo, Japan, Nov. 2002, pp. 371–374.

[47] E. Vourch, B. Della, D. Le Berre, and D. Herve, "Millimeter-wave power-fading compensation for WDM fiber-radio transmission using a wavelength-self-tunable single-sideband filter," *IEEE Trans. Microwave Theory Tech.*, vol. 50, pp. 3009–3015, Dec. 2002.

[48] J. B. Georges, D. M. Cutrer, M.-H. Kiang, and K. Y. Lau, "Multichannel millimeter wave subcarrier transmission by resonant modulation of monolithic semiconductor lasers," *IEEE Photon. Technol. Lett.*, vol. 7, pp. 431–433, Apr. 1995.

[49] H. M. Salgado and J. J. O'Reilly, "Accurate performance modeling of subcarrier multiplexed fiber/radio systems: Implications of laser nonlinear distortion and wide dynamic range," *IEEE Trans. Commun.*, vol. 44, pp. 988–996, Aug. 1996.

[50] C. Lim, A. Nirmalathas, and D. Novak, "Techniques for multichannel data transmission using a multisection laser in millimeter-wave fiber-radio systems," *IEEE Trans. Microwave Theory Tech.*, vol. 47, pp. 1351–1357, July 1999.

[51] B. J. Dixon, R. D. Pollard, and S. Iezekiel, "Orthogonal frequency-division multiplexing in wireless communication systems with multimode fiber feeds," *IEEE Trans. Microwave Theory Tech.*, vol. 49, pp. 1404–1409, Aug. 2001.

[52] I. Seto, H. Shoki, and S. Ohshima, "Optical subcarrier multiplexing transmission for base station with adaptive array antenna," *IEEE Trans. Microwave Theory Tech.*, vol. 49, pp. 2036–2041, Oct. 2001.

[53] A. Kaszubowska, L. P. Barry, and P. Anandarajah, "Multiple RF carrier distribution in a hybrid radio/fiber system employing a self-pulsating laser diode transmitter," *IEEE Photon. Technol. Lett.*, vol. 11, pp. 1599–1601, Nov. 2002.

[54] P. V. Penty, M. Webster, I. H. White, P. Kourtessis, S. D. Walker, and E. J. Tyler, "The applications of SCM in optical datacommunications," in *2002 Int. Topical Meeting Microwave Photonics (MWP2002) Tech. Dig.*, vol. F3–1, Awaji, Hyogo, Japan, Nov. 2002, pp. 363–366.

[55] A. Loayssa, C. Lim, A. Nirmalathas, and D. Benito, "Optical single-sideband modulator for broad-band subcarrier multiplexing systems," *IEEE Photon. Technol. Lett.*, vol. 15, pp. 311–313, Feb. 2003.

[56] G. H. Smith, D. Novak, and C. Lim, "A millimeter-wave full-duplex fiber-radio star-tree architecture incorporating WDM and SCM," *IEEE Photon. Technol. Lett.*, vol. 10, pp. 1650–1652, Nov. 1998.

[57] M. A. Al-numin and G. Li, "WDM/SCM optical fiber backbone for 60 GHz wireless systems," in *2001 Int. Topical Meeting Microwave Photonics (MWP2001) Tech. Dig.*, vol. Tu-2.4, Long Beach, CA, Jan. 2002, pp. 61–64.

[58] Y. C. Chung, "Demonstration of multi-purpose fiber-optic access network (MFAN)," in *2002 Int. Topical Meeting Microwave Photonics (MWP2002) Tech. Dig.*, vol. W3–6, Awaji, Hyogo, Japan, Nov. 2002, pp. 41–44.

[59] T. Kuri, K. Kitayama, and K. Murashima, "Error-free DWDM transmission of 60-GHz-band fiber-radio signals with square-like response fiber Bragg gratings," in *2001 Int. Topical Meeting Microwave Photonics (MWP2001) Tech. Dig.*, vol. Tu-2.6, Long Beach, CA, Jan. 2002, pp. 69–72.

[60] K. Kitayama, T. Kuri, K. Onohara, T. Kamisaka, and K. Murashima, "Dispersion effects of FBG filter and optical SSB filtering in DWDM millimeter-wave fiber-radio systems," *J. Lightwave Technol.*, vol. 20, pp. 1397–1407, Aug. 2002.

[61] H. Toda, T. Yamashita, K. Kitayama, and T. Kuri, "A DWDM millimeter-wave fiber-radio system by optical frequency interleaving for high spectral efficiency," in *2001 Int. Topical Meeting Microwave Photonics (MWP2001) Tech. Dig.*, vol. Tu-3.3, Long Beach, CA, USA, Jan. 2002, pp. 85–88.

[62] ——, "25-GHz channel spacing DWDM demultiplexing for 60-GHz band radio-on-fiber systems using arrayed waveguide grating," in *2002 Int. Topical Meeting Microwave Photonics (MWP2002) Tech. Dig.*, vol. W3–4, Awaji, Hyogo, Japan, Nov. 2002, pp. 33–36.

[63] K. Kikuchi and K. Katoh, "Optical heterodyne receiver for selecting densely frequency division multiplexed signals," *Electron. Lett.*, vol. 38, no. 6, pp. 283–285, Mar. 2002.

[64] ——, "Differential detection of single modulation sideband for ultra-dense optical frequency-division multiplexed systems," *Electron. Lett.*, vol. 38, no. 17, pp. 980–981, Aug. 2002.

[65] T. Okoshi and K. Kikuchi, "Frequency stabilization of semiconductor lasers for heterodyne-type optical communication systems," *Electron. Lett.*, vol. 16, no. 5, pp. 179–181, Aug. 1980.

[66] T. Kuri and K. Kitayama, "Laser phase noise free optical heterodyne detection technique for 60-GHz-band radio-on-fiber systems," in *2000 Int. Topical Meeting Microwave Photonics (MWP2000) Tech. Dig.*, vol. WE1.5, Oxford, UK, Sept. 2000, pp. 141–144.

[67] ——, "Optical heterodyne detection of millimeter-wave-band radio-on-fiber signal with remote dual-mode local light source," *IEEE Trans. Microwave Theory Tech.*, vol. 49, pp. 2025–2029, Oct. 2001.

[68] ——, "Optical heterodyne detection for 60-GHz-band radio-on-fiber systems," *J. Commun. Res. Lab.*, vol. 49, no. 1, pp. 45–56, Mar. 2002.

[69] R. Gross, R. Olshansky, and M. Schmidt, "Coherent FM-SCM system using DFB lasers and a phase noise canceling circuit," *IEEE Photon. Technol. Lett.*, vol. 2, pp. 66–68, 1988.

[70] S. Betti, G. D. Marchis, and E. Iannone, *Coherent Optical Communications Systems*. New York: Wiley, 1995, sec. 9.

[71] T. Kuri and K. Kitayama, "A novel channel selection scheme with optical heterodyne detection using dual-mode local light for DWDM millimeter-wave-band radio-on-fiber systems," in *2002 Int. Topical Meeting Microwave Photonics (MWP2002) Tech. Dig.*, vol. W3–3, Awaji, Hyogo, Japan, Nov. 2002, pp. 29–32.

[72] ——, "A proposal of channel selection scheme of subcarrier multiplexed millimeter-wave-band radio-on-fiber signals with optical heterodyne detection," in *4th Korea-Japan Joint Workshop Microwave Millimeter-Wave Photonics (KJJWS4) Tech. Dig.*, vol. VI-3, Deajeon, Korea, Jan. 2003, pp. 193–196.

[73] T. Okoshi, K. Emura, K. Kikuchi, and R. T. Kersten, "Computation of bit-error-rate of various heterodyne and coherent-type optical communications schemes," *J. Opt. Commun.*, vol. 2, pp. 88–96, Sept. 1981.

[74] G. P. Agrawal, *Nonlinear Fiber Optics*, 2nd ed. New York: Academic, 1995, sec. 2–4.

[75] "A proposal of multiple optical wideband frequency modulation system and its phase noise insensitivity," *IEICE Trans. Fundamentals*, vol. E73-A, no. 9, pp. 1136–1141, Sept. 1995.

Toshiaki Kuri (S'93–M'96) received the B.E., M.E., and Ph.D. degrees from Osaka University, Osaka, Japan, in 1992, 1994, and 1996, respectively.

In 1996, he joined Communications Research Laboratory (CRL), Ministry of Posts and Telecommunications (currently Independent Administrative Institution), Tokyo, Japan, and is mainly engaging in research on optical communication systems.

Dr. Kuri received the 1998 Young Engineer Award from the Institute of Electronics, Information and Communication Engineers (IEICE) of Japan. He is a Member of the IEICE of Japan.

Ken-ichi Kitayama (S'75–M'76–SM'89–F'03) received the B.E., M.E., and Dr.Eng. degrees in communication engineering from Osaka University, Osaka, Japan, in 1974, 1976, and 1981, respectively.

In 1976, he joined the NTT Electrical Communication Laboratory. He spent a year at the University of California, Berkley, as a Visiting Scholar from 1982 to 1983. In 1995, he joined the Communications Research Laboratory, Ministry of Posts and Telecommunications of Japan. Since 1999, he has been a Professor with the Department of Electronic, Information Systems and Energy Engineering, Graduate School of Engineering, Osaka University, Osaka, Japan. His research interests are in photonic networks and radio-on-fiber wireless communications. He has published more than 160 papers in refereed journals, and he has been awarded more than 30 patents.

Prof. Kitayama currently serves on the editorial boards of the IEEE PHOTONICS TECHNOLOGY LETTERS and IEEE TRANSACTIONS ON COMMUNICATIONS. He received the 1980 Young Engineer Award from the Institute of Electronic and Communication Engineers of Japan and the 1985 Paper Award of Optics from the Japan Society of Applied Physics. He is a Member of the Institute of Electronics, Information and Communication Engineers (IEICE) of Japan and the Japan Society of Applied Physics.